Material Properties and Fracture Energy of Kenaf FRP Composites

Zaim Omar[1], Sugiman Sugiman[2], Mustafasanie M. Yussof[3](✉), and Hilton Ahmad[1](✉)

[1] Department of Civil Engineering, Faculty of Civil Engineering and Built Environment, Universiti Tun Hussein Onn Malaysia, 86400 Parit Raja, Johor, Malaysia
hilton@uthm.edu.my

[2] Department of Mechanical Engineering, Faculty of Engineering, University of Mataram, Mataram, Indonesia

[3] School of Civil Engineering, Universiti Sains Malaysia, Engineering Campus, 14300 Nibong Tebal, Penang, Malaysia
gf200067@siswa.uthm.edu.my

Abstract. The incorporations of synthetic fibers have raised worrying concerns, so an alternative material which is inexpensive and ecological resources is proposed. Kenaf fiber has high tensile modulus and elongation at break and potentially to be used as reinforcing fibers in FRP composites to replace synthetic fibers. This study aims to investigate the mechanical properties (unnotched strength, elastic modulus, Poisson's ratio, shear modulus and fracture energy) of woven fabric kenaf fiber-reinforced polymer (KFRP) testing coupons (notched and unnotched), usually employed within numerical modelling. A quasi-static tensile test was performed to investigate the variations of KFRP coupons, such as woven architecture types and KFRP thickness with cross-ply arrangements. Sikadur-31 (epoxy resin) was used as a matrix in KFRP coupons. As kenaf volume fractions and KFRP coupon thickness increased, mechanical properties of KFRP coupons were substantially improved.

Keywords: Natural Fiber · Woven Fabric · Polymer Matrix Composite · Tensile Testing · Material Properties

1 Introduction

The investigation of sustainable engineering materials from agricultural by-products were risen all over the world. This advancement has spurred significantly the industrial partners to create a replacement for synthetic fiber as reinforcing fibers in composite materials [1]. Natural fibers provide favorable environmentally-friendly features, including sustainability, biodegradability, low carbon emissions, non-abrasiveness, recyclability, tensile load resistance cost per weight, and less hazardous handling [2].

Natural fibers are used in a variety of reinforcing fiber class such as continuous, randomly oriented, and woven fabric mats. Excellent integrity, drape-ability and conformability of woven textiles have proven to be more appealing reinforcement types

B. Anshari et al. (Eds.): MIMSE-C-A 2022, AER 215, pp. 223–236, 2023.
https://doi.org/10.2991/978-94-6463-088-6_22

for advanced structural applications [3]. Textile technologies using advanced weaving techniques such as knitting and braiding to create natural fiber-reinforced composites with outstanding mechanical characteristics. The ability of crimps to absorb energy and intercept fractures favors woven fabric kenaf to be more beneficial than unidirectional fibers counterparts [4–6].

Independent measured properties of woven KFRP coupons are very limited in the open literature. This paper presents material properties (i.e., un-notched tensile strength, cohesive fracture energy, tensile elastic modulus, Poisson's ratio, and shear modulus). This research focuses on woven architectural types and KFRP thickness associated with varying numbers of cross-ply woven kenaf layers. The primary goal of this study was to determine the optimization of KFRP plates tested under a quasi-static tensile test.

2 Testing Sets

This section describes testing coupon testing of un-notched coupons and single edge-notch (SEN) coupons, as illustrated in Fig. 1(a) and Fig. 1(b), to measure maximum cohesive strength and fracture energy, respectively. ASTM D 3039/D 3039M-17 [7] was used as the primary reference code of practice throughout the preparation stage and mechanical testing. The KFRP coupon variations included woven architecture types (weaving arrangement and associated fiber counts in warp directions) and KFRP coupon thickness according to stacking woven fabric kenaf layers.

Table 1 shows the KFRP coupons numbers of woven fabric kenaf layers, kenaf volume fraction, V_f (%), coupon thickness, and the number of coupons' designation of testing coupons from series designation investigated. Each un-notched and SEN coupons series (with the notched length of 4, 8 and 12 mm) consist of 12 coupons, respectively. Kenaf fiber yarn was purchased from Bangladesh with a relatively small nominal diameter of 0.75 mm. It has 276 Tex (weight in grams of 1000 m of the tow) with a density of 1.268 g/cm^3 [8]. Kenaf fiber yarn was weaved orthogonally to form a plain-woven fabric layer; this fabric architecture represents a basic woven fabric with a higher crimped rate than other architecture counterparts.

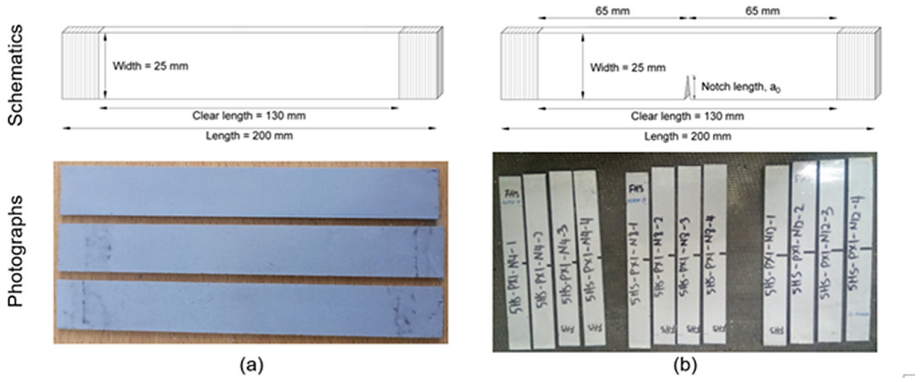

Fig. 1. Geometry of (a) unnotched coupon and (b) single-edge notch (SEN) coupons (Notched with 4-, 8- and 12-mm length).

Table 1. Specimen designations for every set.

Set	Coupons designation	Woven layers'	V_f (%)	Coupon thickness, t_f (*mm*)	No. of coupons			
					Notch length, a_0 (*mm*)			
					0	4	8	12
A	PW4-PX1	1	10	2	3	3	3	3
	PW7-PX1	1	15	2	3	3	3	3
	TW-PX1	1	17	2	3	3	3	3
	5HS-PX1	1	19	2	3	3	3	3
B	PW7-PX1*	1	15	2	3*	3*	3*	3*
	PW7-PX2	2	20	3	3	3	3	3
	PW7-PX4	4	24	5	3	3	3	3

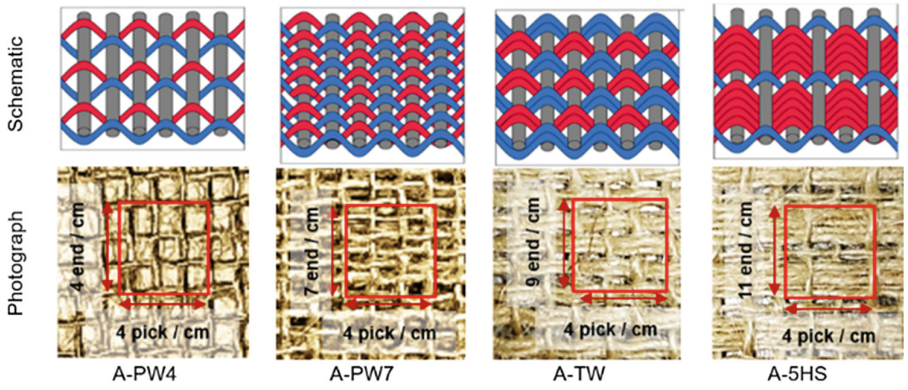

Fig. 2. Weaving architecture patterns conducted in Set A.

As seen in Table 1, Set A comprised four weaving architecture types, i.e., plain weave 4 (PW4), plain weave 7 (PW7), twill weave (TW), and five harness satin (5HS) weaves, each of the patterns has 4, 7, 9 and 11 ends per cm (*epc*) in the warp direction, respectively, and constant four picks per cm (*ppc*) in the weft direction. The coupon designations were labelled as PW4-PX1, PW7-PX1, TW-PX1, and 5HS-PX1, respectively, as shown in Fig. 2. It was seen that kenaf volume fraction increased as yarns in warp direction increased with different of woven architecture types.

Fiber yarn is weaved manually using a rigid plain handloom machine. The term-end and pick described the number of warp and weft tows per unit length in centimeters. The aerial density was made consistent throughout all woven fabric kenaf fibre. The designated density of plain-weave (PW7) fabric of 7 *epc* in the warp direction, while 4 *ppc* in the weft direction. Note that the consistency number of 4 *ppc* is due to the constant designated hole of the handloom machine in the orthogonal warp direction.

Set B concentrated on nominal KFRP thickness respective to the number of cross-ply layers (2 mm (1 layer), 3 mm (2 layers) and 5 mm (4 layers)) and labelled as PW7-PX1, PW7-PX2, and PW7-PX4, respectively. The kenaf volume fraction in KFRP coupons was low respective to kenaf fabric layers, giving an adverse effect on the kenaf volume fraction. PW7-PX1 has identical specimens of previously in Set-A.

3 KFRP Coupons Preparations

This section elaborates on the preparation stage of woven fabric KFRP coupons according to the testing sets investigated. The epoxy resin was used with a commercial brand of Sikadur-31 SBA S-02 (SK31). The guideline in handling SK31 was referred to Material Safety Data Sheet (MSDS) from Sika. The density, shear strength, and elastic modulus for blended epoxy resins are 1.80 kg/l, 12.0 MPa and 8000 MPa, respectively. The color appearance of SK31 is concrete grey with a mixing ratio of 3:1 (Epoxy:Hardener). The hardener was added to the epoxy resin to accelerate the setting time of the blended matrix system with a specified mixing ratio.

The fabrication of KFRP coupons was elaborated as follows. The molding coupon is inspected to be clean and free from contaminations to provide smooth and even surface finishing panels. The desired thickness and sizes of composite panels were controlled by the aluminum plate thickness, which was used as railing edges surrounding the fabricated panel. The fabrication process was started by applying a thin layer of silicon spray on both the top and bottom aluminum mold as a release agent. An epoxy resin was smeared on mold as the first layer followed by a woven fabric kenaf was placed and pressed uniformly to ensure woven kenaf was wetted by epoxy resin. These steps were repeated accordingly until desired stacking sequences were achieved as specified in the experimental testing sets. Epoxy resin of top layer was smeared and levelled uniformly, and then the laminate was covered by an aluminum plate. The laminate was left for curing for at least 24 h at room temperature under a constant load of 100 kg. Having cured, the aluminum molds were carefully removed to avoid premature damage of the composite panel surface.

The fabricated woven KFRP composite panels with 250 mm length and 230 mm width were sectioned into the desired coupon by using an electric cut-off machine. SEN coupons were introduced by making a notched at the coupon centerline according to designated notch heights (4, 8 and 12 mm). Sandpaper was used to polish the cut edge surfaces and aluminum plates were glued to the end tab for better gripping. Testing coupons with little or no voids were carefully selected for further experimental work. The coupon geometries such as coupon width, thickness and notch height were measured using a digital vernier caliper and recorded accordingly.

4 Preparations KFRP Coupons Testing Set-Ups

Mechanical testing was used to determine in-plane modulus elasticity, Poisson ratio, shear modulus, unnotched strength and fracture energy. The mechanical testing was carried out using a Universal Testing Machine (UTM) machine with 50 kN load-cell capacity and a constant crosshead speed rate of 0.5 mm/min. The low testing rate was intended to provide sufficient time for crack tip propagation detection and to prevent

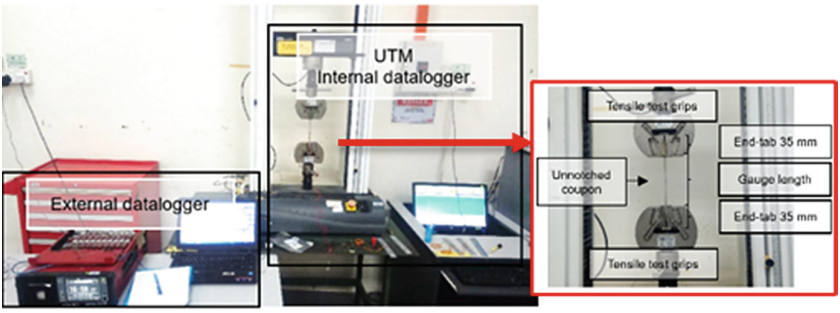

Fig. 3. KFRP coupons tensile test set-up.

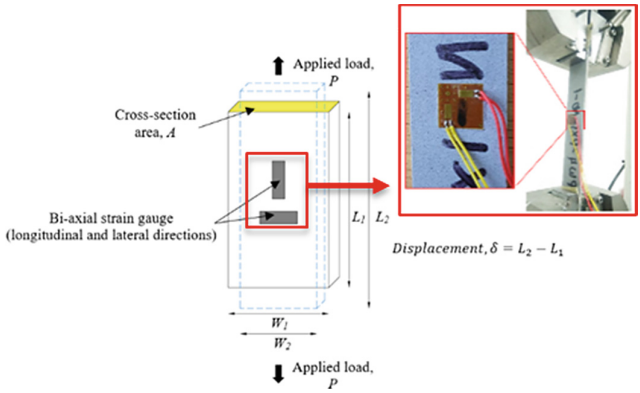

Fig. 4. Schematic strain measurement by using strain gauge using tensile test set-up configuration.

sudden catastrophic failure in the beam specimens. The data logger cycle interval (sampling rate) was taken as 1.0 pts/s. The data acquisition system collects and analyses the load-deflection data.

4.1 Determination of Material Properties

The un-notched coupons tests were carried out by using UTM machine to independently determine elastic and material properties, including young's modulus, Poisson ratio, shear modulus and un-notched strength in longitudinal and transverse directions. Figure 3 shows an unnotched coupon under tensile test set-up, where unnotched strength were recorded by UTM machine internal data logger and elastic modulus was calculated by measuring the slope of stress-strain at the elastic region.

Meanwhile, Poisson's ratio value was determined by biaxial strain gauge data mounted at the centerline in both longitudinal and lateral directions. An active gauge length and gauge factor of 3 mm and 2.08 were bonded to the centerline of unnotched coupons using a cyanoacrylate adhesive (see Fig. 4). The biaxial strain gauge was positioned orthogonally upon KFRP unnotched coupons.

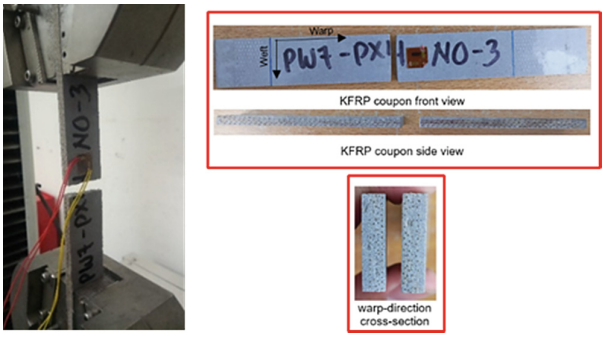

Fig. 5. Failure occurred within gauge length on KFRP unnotched coupon.

Strain increment profile datasets were recorded and extracted from UTM machine data-logger to obtain longitudinal and lateral strains for Poisson's ratio calculations. Longitudinal and lateral strain was obtained from Eq. (1) and Eq. (2), respectively. As the applied load increased, deformations in both orthogonal directions to exhibit elongation and shortening of unnotched coupon in longitudinal and lateral directions, respectively. Poisson's ratio was calculated from Eq. (3) were taken between 0.05% and 0.3% strain interval as obtained from data-logger.

$$\varepsilon_{lateral} = \varepsilon_x = \frac{W_2 - W_1}{W_1} \times 100\% \tag{1}$$

$$\varepsilon_{longitudinal} = \varepsilon_y = \frac{L_2 - L_1}{L_1} \times 100\% \tag{2}$$

$$\upsilon_{xy} = -\frac{\varepsilon_x}{\varepsilon_y} \tag{3}$$

At least three coupons were prepared for each testing series laminates. Young's modulus was taken within vertical strain internal of 0.1% and 0.2% from respective stress-strain curve. All the tested unnotched coupons presented failure break within the gauge length as shown in Fig. 5, where the KFRP damage can be visually seen with naked eyes. Due to no coupon discontinuities, the coupons tend to break at the griping region due stress concentration at the edge grip. If this occurred, the respective coupons were discarded and repeated until the coupon demonstrated failure within its gauge length.

Another independent elastic property to be determined was the shear modulus of all testing series designation by referring to ASTM D2344/D2344M-16 [9]. Shear modulus was highly dependent upon the nature of fiber orientation where cross-ply lay-up was determined by testing unnotched coupons with diagonal cut at 45° to woven fabric fiber orientation. A similar procedure was implemented as discussed previously, to determine Poisson's ratio value where bi-linear strain gauge were positioned at mid-line of KFRP coupon. Maximum principal shear stress occurred at an angle of 45°, therefore this is regarded as the optimum angle of fibers to resist shear and placed diagonally. The strain values were recorded by the external data logger, and shear modulus was determined by Eq. (4) [10] where ε_y is longitudinal strain and ε_x is the lateral strain (extracted from

connected data-logger). In addition, σ_{ult} is the applied stress at failure from Eq. (5) where P_{ult} is applied load at failure and A is the cross-section area.

$$G_{xy} = \frac{\sigma_{ult}}{2(\varepsilon_y - \varepsilon_x)} \tag{4}$$

$$\sigma_{ult} = \frac{P_{ult}}{A} \tag{5}$$

4.2 Determination of Cohesion Fracture Energy

Critical strain energy release rate, also known as fracture energy (G_c), was measured using SEN coupons according to ASTM E399-22 [11]. The SEN testing coupons were prepared, and sharp edge notches was sectioned by using jig saw for each millimeter (mm) of notch length. Correspondingly, three testing coupons were allocated to determine maximum fracture load, P_{ult} for each notch length specified (4 mm, 8 mm, and 12 mm) to give of nine coupons required for each testing set. After testing the SEN, the relationship between coupon compliance and notch length was plotted to obtain fracture energy.

Fracture energy was obtained from using Eq. (6) where P_{ult} represented the ultimate load at failure of the respective SEN coupon. B is coupon thickness, C is coupon compliance, and a is the notch length of the edge notch. Load-displacement profile for each notch length was plotted to determine associated coupon stiffness, k. Stiffness was obtained from the respective load-displacement slope and taken inversely to obtain the respective compliance of the testing coupon, C as given in Eq. (7). The compliance against notch length graph was plotted, and the second order polynomial expression was differentiated to obtain dC/da from Eq. (6) [10]. Then, fracture energy was taken by averaging fracture energy of 4 mm, 8 mm, and 12 mm notch length.

$$G_c = \frac{P_{ult}^2}{2B}\frac{dC}{da} \tag{6}$$

$$C = \frac{1}{k} \tag{7}$$

Figure 6 displays an illustration of a load-displacement graph created using data from an SEN coupon (PW4-PX1). As shown in Fig. 6, a sample calculation was used to calculate the stiffness *(k)* and compliance *(C)* of the testing coupon between the displacement intervals of 0.03 mm and 0.40 mm A graph of compliance against notch length was produced, and a typical curve was presented as shown in Fig. 7 for PW4-PX1 SEN coupons. A second-order polynomial expression was used to create the curve with a rising trend of notch length increments to its respective compliance and notch length. Then, this expression was implemented in Eq. (6) upon first differentiation of dC/da to calculate the fracture energy in each designed lay-up series.

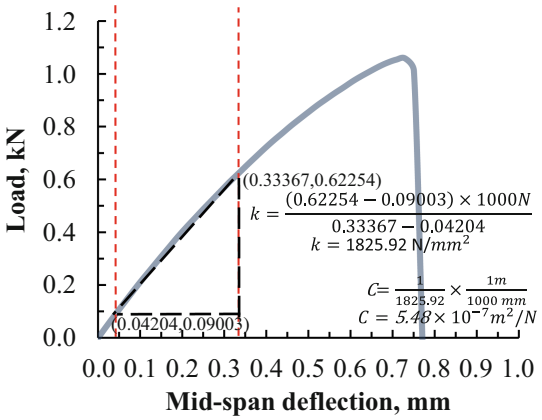

Fig. 6. Load-displacement graph plotted to determine stiffness and compliance from specimen PW4-PX1 with notch length of 4 mm.

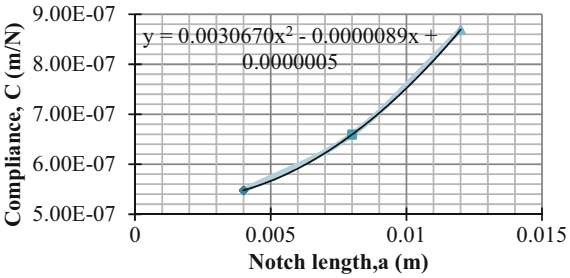

Fig. 7. Graph of compliance against notch lengths (PW4-PX1).

5 Result and Discussion

In the current study, three testing specimens were tested, and good reproducibility was found. Figure 8 shows the representative stress-strain curves on unnotched KFRP coupons. The stress-strain curves demonstrates that elastic slope decreased and unnotched strength increased as the kenaf volume fraction increased.

The measured material properties are given in Table 2. Figure 9 shows gradually increased averages of unnotched strength where 5HS-PX1 exhibited the highest unnotched strength than TW-PX1, PW7-PX1 and PW4-PX1 counterparts within Set A series. As expected, more yarn fibers in warp direction are able to sustain more applied load as the direction is the most effective loading resistance angle to the loading direction. Meanwhile, PW7-PX4 shows the highest unnotched strength. Respective of coupon thickness, thicker coupons have better-unnotched strength than thinner counterparts (PW7-PX1 and PW7-PX2) due to better out-of-plane resistance throughout the coupon thickness. This is because thicker coupon has more reinforcing layers and is associated with higher delamination resistance.

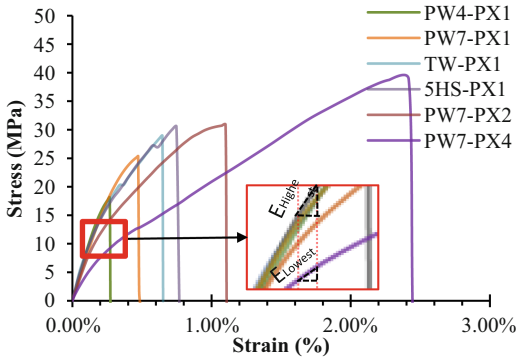

Fig. 8. Stress-strain curves.

Table 2. Material properties of unnotched cross-ply woven fabric KFRP coupons.

Specimen Name	Coupon	Unnotched strength, σ_0 (MPa)	Mean σ_0 (MPa)	Elastic Modulus, E_x (MPa)	Mean E_x (MPa)	Poisson Ratio, υ_{xy}	Mean υ_{xy}
PW4-PX1	1	18	17.7	6617	6688	0.181	0.185
	2	18	± 0.4	6856	± 146	0.183	± 0.006
	3	17		6592		0.192	
PW7-PX1	1	25	25.0	6055	6212	0.219	0.214
	2	25	± 0.4	6159	± 189	0.213	± 0.005
	3	25		6422		0.209	
TW-PX1	1	29	28.8	6055	6034	0.229	0.225
	2	28	± 0.6	5891	± 134	0.221	± 0.004
	3	29		6156		0.225	
5HS-PX1	1	30	30.6	5955	5877	0.231	0.237
	2	31	± 0.8	5921	± 107	0.241	± 0.005
	3	31		5755		0.238	
PW7-PX2	1	31	31.8	4710	4638	0.254	0.254
	2	31	± 1.3	4625	± 67	0.247	± 0.007
	3	33		4579		0.262	
PW7-PX4	1	40	38.2	2776	2871	0.283	0.277
	2	39	± 2.2	3072	± 174	0.275	± 0.005
	3	36		2765		0.273	

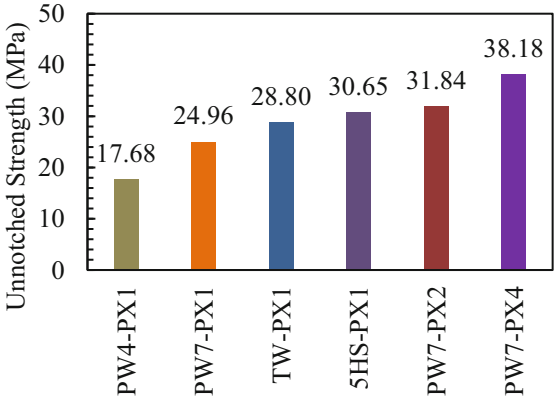

Fig. 9. Unnotched strength KFRP unnotched coupons.

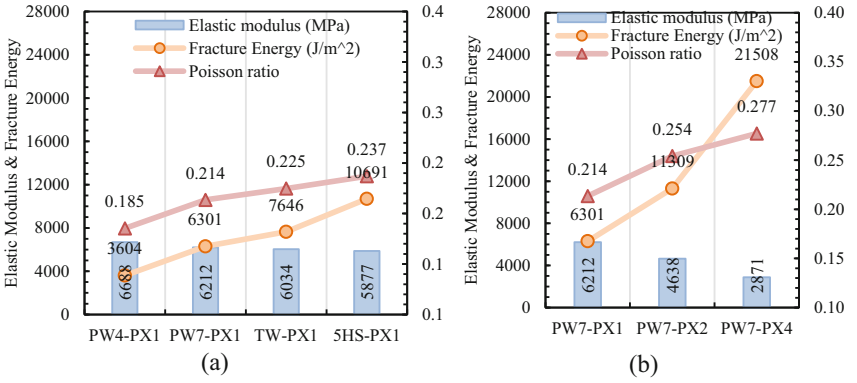

Fig. 10. Effect of woven fabric kenaf (a) architecture lay-up (b) layer and coupon thickness.

Figures 10 show elastic modulus, Poisson ratio and fracture energy for Set A and Set B. From Fig. 10, PW4-PX1 has a higher elastic modulus than PW7, TW and 5HS. Furthermore, the thickest coupon (PW7-PX4) has the lowest elastic modulus value. This is associated with lower deformation (or lower strain) in thinner coupons to promote a steeper stress-strain curve. Bear in mind, the elastic modulus for epoxy resin is 8000 MPa as stated in MSDS. The introduction of woven fabric kenaf prone to reduce elastic modulus in epoxy resin resulting from fiber volume fraction contribution. This elastic modulus trends showing a good agreement with Cuenot et al. [12] and Sharpe et al. [13].

The low coefficient of Poisson's ratio was given with the least volume fraction content (PW4-PX1) compared to other six KFRP coupons, and interactions between the deformation of materials of architecture types, and KFRP thickness is relatively small. The Poisson ratio results demonstrated greater composite flexibility as the Poisson ratio is higher [14].

Table 3 tabulated shear modulus of unnotched quasi-isotropic woven fabric KFRP coupons. The architecture types showed that 5HS-PX1 has the higher shear modulus

Table 3. Shear modulus of unnotched quasi-isotropic woven fabric KFRP coupons.

Specimen Name	Coupons	Shear modulus, G_{xy} (MPa)	Mean G_{xy} (MPa)
PW4-PX1	1	496	508
	2	518	± 12
	3	511	
PW7-PX1	1	591	585
	2	594	± 12
	3	572	
TW-PX1	1	612	616
	2	602	± 17
	3	635	
5HS-PX1	1	654	650
	2	666	± 19
	3	630	
PW7-PX2	1	725	697
	2	693	± 27
	3	673	
PW7-PX4	1	772	760
	2	787	± 35
	3	721	

than PW4-PX1, PW7-PX1, and TW-PX1, to withstand larger shear deformation and increase its shear stiffness. The stacking sequences of specimens PW7-PX1, PW7-PX2, and PW7-PX4 lay-ups were like increased interfacial resistance, resulting from reducing delamination failure. The matrix epoxy resin (SK-31) is an effective binder to woven fabric kenaf fibers because of its high viscosity and ability to be thoroughly absorbed by crimped fibers.

U-shape edge notches were introduced to every 4 mm interval notch length, ranging from 4, 8 and 12 mm and tested to failure. The maximum load was taken as failure load of testing coupons in the respective notched length, similar approach used in Belmonte [10] and Lee & Ahmad [15]. The maximum load of SEN coupons tested was averaged from the triplicate testing coupons and fracture energy in each notch length specified were tabulated in Table 4. In Set A, higher crimping regions prone to increase fracture energy by delaying damage to the respective KFRP coupon. On the contrary, in set B showed gradual steep trends of fracture energies. The fracture energy shows increasing, which are 6.3 kJ/m^2, 11.3 kJ/m^2 and 21.5 kJ/m^2 in testing coupons with designations of PW7-PX1, PW7-PX2 and PW7-PX4, respectively. It was found that thickest lay-up and largest volume of fiber yarns in warp direction promotes optimum fracture energy

Table 4. Fracture energies of SEN KFRP coupons.

Specimen Name	Notch length, a (mm)	Maximum load, P_{max} (N)	G_c (J/m^2)	Mean G_c (J/m^2)
PW4-PX1	4	1066	3917	
	8	643	3726	3604
	12	466	3169	
PW7-PX1	4	1290	5897	
	8	964	8314	6301
	12	566	4694	
TW-PX1	4	1351	5396	
	8	993	9401	7646
	12	699	8141	
5HS-PX1	4	1425	7661	
	8	1073	13258	10691
	12	742	11154	
PW7-PX2	4	1559	11436	
	8	1330	13916	11309
	12	886	8576	
PW7-PX4	4	3182	22621	
	8	2360	23307	21508
	12	1801	18596	

value. Guedes [16] also reported that thicker coupons have higher fracture energy than thinner coupon's counterpart.

6 Concluding Remarks

Testing sets and associated effects were investigated, and careful measurements were made. Through this paper, 72 specimens (unnotched coupons and SEN coupons) were produced and successfully tested under quasi-static tensile testing. Various series of KFRP coupons were fabricated to evaluate their performances and associated deformations. Generally, the testing sets results indicate that all KFRP coupons have significantly improved the material properties when architecture woven fabric kenaf arrangements and KFRP coupon thickness increases. The effects of architecture types improved in plain weave with 7 epc warp direction. Additionally, the thickest KFRP coupon gave good tension resistance due to inter-laminar strength between its adjacent layers.

Acknowledgement. This research was financially supported by Ministry of Higher Education Malaysia (MOHE) through Fundamental Research Grant Scheme (FRGS/1/2020/

TK01/UTHM/02/4). We also want to thank Research Management Centre (RMC), University Tun Hussein Onn Malaysia (UTHM), for sponsoring this work under Postgraduate Research Grant (GPPS) (Research Grant No. H685).

References

1. A. N. Nayak, A. Kumari, and R. B. Swain.: Strengthening of RC Beams Using Externally Bonded Fiber Reinforced Polymer Composites. Structures, vol. 14, no. December 2017, pp. 137–152 (2018).
2. L. Ying, T. Gao, W. Hou, M. Dai, X. Han, and D. Jiang Specimen fabrication: On crashing behaviors of bio-inspired hybrid multi-cell AL/CFRP hierarchical tube under quasi-static loading: An experimental study. *Compos. Struct.*, no. August, p. 113103 (2020).
3. D. Tholibon, A. B. Sulong, N. Muhamad, D. A. Tholibon, I. Tharazi, and N. F. Ismail.: Tensile Properties of Unidirectional Kenaf Polypropylene Composite at Various Temperatures and Orientations. vol. 890, pp. 16–19 (2017).
4. R. Mahjoub, J. M. Yatim, A. R. Mohd Sam, and S. H. Hashemi: Tensile properties of kenaf fiber due to various conditions of chemical fiber surface modifications. *Constr. Build. Mater.*, vol. 55, pp. 103–113 (2014).
5. O. Faruk, A. K. Bledzki, H. P. Fink, and M. Sain: Biocomposites reinforced with natural fibers: 2000–2010. *Prog. Polym. Sci.*, vol. 37, no. 11, pp. 1552–1596 (2012).
6. M. R. Ishak, Z. Leman, S. M. Sapuan, A. M. M. Edeerozey, and I. S. Othman: Mechanical properties of kenaf bast and core fiber reinforced unsaturated polyester composites. IOP Conf. Ser. Mater. Sci. Eng., vol. 11, p. 012006 (2010).
7. ASTM standard D3039/D3039M-17: Standard test method for tensile properties of polymer matrix composite materials (2017).
8. S. Y. Lee: Experimental Study and Numerical Modelling of Woven Fabric Kenaf Fiber Composites Hybrid Adhesively Bonded-Bolted Joints. Universiti Tun Hussein Onn Malaysia: Ph.D. Thesis (2018).
9. ASTM standard D2344/D2344M-16: Standard Test Method for Short-Beam Strength of Polymer Matrix Composite Materials and Their Laminates (2016).
10. H. M. S. Belmonte.: Notched Strength of Woven Fabric Composites. University of Surrey: Ph. D Thesis (2002).
11. ASTM standard E399-22: No Title Standard test method for plane-strain fracture toughness of metallic materials (2022).
12. S. Cuenot, C. Frétigny, S. Demoustier-Champagne, and B. Nysten: Surface tension effect on the mechanical properties of nanomaterials measured by atomic force microscopy. Phys. Rev. B - Condens. Matter Mater. Phys., vol. 69, no. 16, pp. 1–5 (2004).
13. W. N. Sharpe, K. M. Jackson, K. J. Hemker, and Z. Xie: Effect of specimen size on young's modulus and fracture strength of polysilicon. J. Microelectromechanical Syst., vol. 10, no. 3, pp. 317–326 (2001).
14. R. Bhowmik, S. Das, D. Mallick, and S. S. Gautam: Predicting the elastic properties of hemp fiber - A comparative study on different polymer composite. Mater. Today Proc., vol. 50, pp. 2510–2514 (2021).
15. L. S. Yee and H. Ahmad: XFEM modelling of single-lap Kenaf fiber composite hybrid joints under quasi-static loading. Plast. Rubber Compos., vol. 48, no. 2, pp. 48–56 (2019).
16. R. M. Guedes: Validation of trace-based approach to elastic properties of multidirectional glass fiber reinforced composites. *Compos. Struct.*, p. 113170 (2020).